

Lower bounds on dark matter annihilation cross-sections by studying the fluctuations of 21-cm line with dark matter candidate in inert doublet model (IDM) with the combined effects of dark matter scattering and annihilation

Rupa Basu^{*} and Shibaji Banerjee[†]

Department of Physics, St. Xavier's College, 30, Mother Teresa Sarani, Kolkata-700016, India.

Madhurima Pandey[‡] and Debasish Majumdar[§]

Astroparticle Physics and Cosmology Division,

Saha Institute of Nuclear Physics, HBNI

1/AF Bidhannagar, Kolkata-700064, India.

(Dated:)

We study the fluctuations in the brightness temperature of 21-cm signal δT_{21} focused at the dark age ($z \sim 100$) with dark matter candidate in IDM model for the two cases where (1) the dark matter (DM) relic densities Ω_c lie within the 95% confidence limit of the relic density $\Omega_{c,0}$ obtained from the Planck experiment and (2) the values of Ω_c are not comparable with $\Omega_{c,0}$. We consider both the DM annihilation and the DM-baryon elastic scattering as the combined additional effect on δT_{21} in the presence of thermal evolution. We find the absorption spectra of δT_{21} for the case (1) whereas we see the emission spectra of δT_{21} for the case (2). This imposes a lower bound on the DM annihilation cross-sections which lie in the range $6.5 \times 10^{-29} \text{ cm}^3/\text{sec} \leq \langle \sigma v \rangle \leq 4.88 \times 10^{-26} \text{ cm}^3/\text{sec}$ for the DM mass range $10 \text{ GeV} \leq M_\chi \leq 990 \text{ GeV}$. We also see that δT_{21} follows DM-baryon elastic scattering for $10 \text{ GeV} \leq M_\chi \leq 60 \text{ GeV}$ and DM annihilation for $70 \text{ GeV} \leq M_\chi \leq 990 \text{ GeV}$. We also find that for the dark matter mass range (in the framework of IDM model) $10 \text{ GeV} \leq M_\chi \leq 60 \text{ GeV}$, DM-baryon elastic scattering is more relevant for producing δT_{21} while for the dark matter mass range of $70 \text{ GeV} \leq M_\chi \leq 990 \text{ GeV}$ dark matter annihilation is more favoured for explaining δT_{21} .

^{*} rupabasu.in@gmail.com

[†] shiva@sxccal.edu

[‡] madhurima.pandey@saha.ac.in

[§] debasish.majumdar@saha.ac.in

I. INTRODUCTION

The cosmic dark ages that span between the era of recombination leading to thermal decoupling of baryons from photons at $z \simeq 1100$ upto the era of re-ionization with ignition of first stars at around $z \sim 20$ could serve as a sensitive probe for any source of energy input into the cosmos. After recombination, the CMB temperature and the matter temperature remains in the same order due to Compton scattering of the residual electrons. But after $z \sim 150$ due to adiabatic expansion, the matter temperature T_b goes as $T_b \propto (1+z)^2$. In case T_b deviates from this dependence, it would indicate the presence of other sources of energy injection (or absorption). The measurement of brightness temperature of 21-cm Hydrogen line could be such a probe [1–3].

The 21-cm hydrogen line originates due to the hyperfine transition between triplet ($S = 1$) and singlet ($S = 0$) states in hydrogen atom. The triplet state manifests when the nuclear spin and the electron spin of the hydrogen atom are aligned in contrast, the singlet state corresponds to the state when two spins are antiparallel. The strength of the transition is defined in terms of the populations of triplet and singlet states (n_1 and n_0 respectively) and the spin temperature T_s of the baryon gas [4] can be described as

$$\frac{n_1}{n_0} = 3 \exp\left(-\frac{T_*}{T_s}\right) \simeq 3 \left(1 - \frac{T_*}{T_s}\right), \quad (1)$$

where $T_* = 0.068$ K represents the energy corresponding to the 21-cm transition (energy difference between the spin states $S = 0$ and $S = 1$ of ground state hydrogen). At $z \sim 20$ when the first star ignites, the UV radiation from this ignition initiates transitions from triplet to singlet state of hydrogen through Wouthuysen-Field effect [5] and the spin temperature tends to be equal to the baryon temperature. The temperature of the 21-cm line redshifted to today is defined as the brightness temperature of 21-cm line [1–3] in the background of CMB, given by

$$\delta T_{21} = \frac{T_s - T_\gamma}{1+z} (1 - e^{-\tau}) \simeq \frac{T_s - T_\gamma}{1+z} \tau, \quad (2)$$

where T_γ is the CMB temperature and τ is the optical depth. The spin temperature T_s is smaller than the CMB temperature during dark age. So the brightness temperature of 21-cm line gives a negative value at this epoch. As an example, at $z \sim 20$ the brightness temperature of 21-cm line is $\delta T_{21} \sim -209$ mK. But the EDGES [6] experiment measured 21-cm absorption features with brightness temperature $\delta T_{21} = -500^{+200}_{-500}$ mK at 100 MHz frequency. This unexpected cooling may be either due to the baryon temperature is cooler than expected or there are other 21-cm sources. We adopt the first possibility in this work considering the proposition that, the cooling has been effected by the interaction of dark matter with the baryon. Also dark matter (DM) annihilation can inject energy into the system [7, 8] thereby influence the features of δT_{21} brightness.

In this work we choose the particle dark matter candidate by considering an well established particle dark matter model namely Inert Doublet Model (IDM) [9–11] in which the Standard Model of particle physics (SM) is minimally extended by adding an extra doublet scalar. With this particle dark matter we compute the heating rates for dark matter, baryons etc. relevant for calculation of δT_{21} brightness by solving a set of coupled differential equations. Also the annihilation of these DM particles from the models given above are studied in the context of the brightness temperature δT_{21} of the absorption line [12]. There are number of literatures discuss the viability of IDM to be a dark matter candidate [10, 11].

In the IDM model an extra inert Higgs is added with the Standard Model. This additional scalar SU(2) doublet does not acquire any vacuum expectation value (vev) on spontaneous symmetry breaking (SSB). A discrete Z_2 symmetry is imposed on the added scalar such that the added doublet is Z_2 even while the SM is Z_2 odd. Thus it does not mix with SM Higgs. This ensures that the stability of the added scalar and also insures that it has no interaction with SM fermions. The lighter of the two scalars of this inert doublet is then the candidate for dark matter. Initially motivated to address the problem of quadratic divergence in Higgs sector and to solve naturalness problem, the added doublet can well be a viable candidate of particle dark matter. This additional doublet neither develops a vacuum expectation value (vev) on spontaneous symmetry breaking (SSM) nor it has any interaction or coupling with Standard Model Fermions. So the model contains two doublet scalars. One is the usual Standard Model Higgs doublet H_1 and the other is H_2 . The decoupling of H_2 with SM fermions is complete by imposing a discrete Z_2 symmetry such that under this symmetry $H_2 \rightarrow -H_2$ while other fields remain invariant. After SSB the vev of the two scalar fields are $H_1 = (0, v)$ and $H_2 = (0, 0)$ and on expanding around the minima one obtains

$$H_1 = \begin{pmatrix} \phi^+ \\ v + (h + i\chi) \end{pmatrix}, \quad H_2 = \begin{pmatrix} H^+ \\ (S + iA)/\sqrt{2} \end{pmatrix},$$

where both S and A can be dark matter candidates.

In this analysis we use IDM model and estimate the fluctuation in the brightness temperature of 21-cm signal for the two cases where (1) the relic densities lie within 95% confidence limit of the relic density obtained from the Planck experiment [13] and (2) the relic densities does not comparable with the relic density obtained from the Planck experiment [13]. In both cases we study the DM annihilation [7, 8, 14, 15] and DM-baryon elastic scattering [16, 17] in the presence of thermal evolution effect on the fluctuation of the brightness temperature of 21-cm signal. A brief outline of the paper follows. In the Section II we discuss the formalism considered in this analysis. Section III shows the results and we summarize and conclude our findings in Section IV.

II. FORMALISM

Recent EDGES experiment [6] detects the global 21-cm signal with some uncertainties. The fluctuation in 21-cm signal is quantified by its differential brightness temperature δT_{21} , which depends on the spin temperature T_S , CMB temperature T_γ and optical depth τ (Eq. 2). The spin temperature T_S is the excitation temperature of 21-cm line which depends on the ratio of population number density of the two hyperfine splitting of hydrogen atom and that can be estimated using Eq. 1. Further we approximate T_S [4, 18] by neglecting the Wouthuysen-Field effect [5] as

$$T_S = \frac{(T_\gamma A_{10} + C_{10} T_\star) T_b}{A_{10} T_b + C_{10} T_\star} \quad (3)$$

where $T_\star = hc/k\lambda_{21\text{cm}} = 0.068\text{K}$, $A_{10} = 2.85 \times 10^{-15} s^{-1}$ is the Einstein coefficient and C_{10} is the collisional transition rate [19].

From Eqs. 2 and 3, it is clearly noted that the fluctuation in the brightness temperature of 21-cm signal depends on the baryon temperature. Thermal evolution in the universe evolves the baryon temperature T_b . In this analysis, we consider DM annihilation and DM-baryon elastic scattering as the additional contributions to the evolution of T_b , which is given by

$$\frac{dT_b}{da} = -2 \frac{T_b(a)}{a} + \frac{\Gamma_c(a)}{a H(a)} (T_\gamma(a) - T_b(a)) + \frac{2}{3 a H(a)} \frac{f_{heat}}{(1 + f_{He} + x_e) n_H} \left(\frac{dE}{dV dt} \right)_{inj} + \frac{2}{3 a H(a)} \left(\frac{dQ_b}{dt} \right) \quad (4)$$

where $H(a)$ is the Hubble parameter and Γ_c is the Compton scattering rate, x_e is the number of free electron and f_{He} is the relative number of abundance of the helium nuclei. For the simplicity of the calculation we consider $x_e = 2 \times 10^{-4}$ and $f_{He} = n_{He}/n_H$. $dE/(dV dt)_{inj}$ is the energy injection rate per unit volume and dQ_b/dt is the heating rate of the baryons in their rest frame. The third term of Eq. 4 represents the DM annihilation effect whereas the fourth term of Eq. 4 represents the DM-baryon elastic scattering effect. In the later part of this section we discuss these two additional effects in detail.

The term Γ_c arises in Eq. 4 due to the scattering between CMB photons and residual free electrons. The number density of CMB photons is much larger than the residual free electrons, which implies that the Compton scattering of CMB photons with the residual free electrons is much more efficient to keep the baryon in thermal equilibrium with CMB photons. Hence the Compton scattering rate Γ_c depends on the number of free electrons x_e and this is given by

$$\Gamma_c = \left(\frac{8 \sigma_T a_r T_\gamma^4}{3 m_e} \right) \frac{x_e}{1 + f_{He} + x_e} \quad (5)$$

where σ_T is the Thomson cross-section, a_r is the radiation constant and m_e is the mass of electron.

We now discuss the DM annihilation as an additional effect in the evolution of the baryon temperature T_b . DM annihilation heats the baryon and increases the baryon temperature T_b . We have discussed earlier that a higher T_b modifies the fluctuation in T_{21} spectrum. The heating of baryons by DM annihilation proceeds through two mechanisms. The first one is during the epoch of thermal decoupling from CMB. In this case DM annihilation increases the number of free electrons above the threshold value predicted by the standard model [14], *i.e.* $x_e = n_e/n_b \approx 2 \times 10^{-4}$. A large value of x_e delays the CMB decoupling and as a result this increases T_b since the baryon has less time to cool adiabatically. The second mechanism involves injection of energy when DM annihilation directly heats the baryon and increases T_b . We have discussed earlier that the third term of Eq. 4 represent the DM annihilation contribution to the evolution of T_b .

The energy injection rate per unit volume $dE/(dV dt)_{inj}$ is estimated by assuming that DM annihilates to standard model particles and injects energy into the universe [14]. This process further drives the additional ionization, excitation and heating of the gas. For a given velocity averaged annihilation cross-section $\langle \sigma v \rangle$, $dE/(dV dt)_{inj}$ is given by

$$\left(\frac{dE}{dV dt} \right)_{inj} = \rho_\chi^2(a) B(a) f_\chi^2(a) \frac{\langle \sigma v \rangle}{M_\chi} \quad (6)$$

where f_χ is the fraction of the dark matter which annihilates to standard model particles and ρ_χ is the dark matter mass density. In the above, $B(a) = 1 + 1.6 \times 10^5 a^{1.54} \text{Erfc}(\frac{1}{20.5a})$ is the boost factor as prescribed by [14]. The injected energy deposited in the baryon mainly in three different ways, *viz.* ionization, excitation and heating [14]. The dimensionless quantity f_{heat} in Eq. 4 represents the efficiency of energy deposition in the baryon by heating. f_{heat} depends on the DM mass and this includes the time delay between the deposition and injection of energy. In this analysis we consider SSCK approximation [14] to estimate f_{heat} , which is given by

$$f_{heat} = f_{eff} \left(\frac{1 + 2x_e}{3} \right) \quad (7)$$

where f_{eff} is the fraction of the energy produced by DM annihilation immediately transferred to the plasma. Following [20, 21] we adopt the values of f_{eff}^1 for the photons and the e^+e^- pairs injected at keV-TeV energies.

We now discuss the DM-baryon elastic scattering as an additional effect in the evolution of the baryon temperature T_b . The interaction between DM and baryons changes their temperature and add contribution to the evolution of baryon temperature T_b . This interaction process not only responsible for the cooling of baryons but also heating. In general during the interaction between two fluids (say DM and baryons), the hot fluid lose its energy to the colder one and there will be no transfer of energy if both the fluids have same temperature. According to [16], if there is a relative velocity between the two fluids then there should be an additional term of friction which will tend to damp the motion and the kinetic energy lost in this fashion will increase the temperature of both fluids. In Ref.[16], it has been shown that the magnitude of this interaction effect depends on the initial relative velocity which is a Gaussian variable with variance of $\sim 29 \text{ km s}^{-1}$ at $z = 1010$.

We follow the methodology prescribed in [16] to estimate the quantity dQ_b/dt (Eq. 4), the heating rate of the baryons in their rest frame. The interaction between DM and baryons at different temperature heats up the cold dark matter and try to keep their temperature in equilibrium, where the heating rate is proportional to the temperature difference. However if there is a relative velocity between DM and baryons then the friction term heats up both DM and baryons irrespective of their temperature difference. Using Eq. 16 of Ref. [16] the heating rate of baryon is given by

$$\frac{dQ_b}{dt} = \frac{2m_b\rho_\chi\sigma_0 e^{-\frac{v^2}{2}} (T_\chi - T_b)^3}{(m_\chi + m_b)^2 \sqrt{2\pi} u_{th}} + \frac{\rho_\chi}{\rho_m} \frac{m_\chi m_b}{m_\chi + m_b} V_{\chi b} \left(\frac{dV_{\chi b}}{dt} \right) \quad (8)$$

where m_χ and m_b are the masses of DM and baryon respectively. ρ_χ is the energy density of DM, ρ_b is the energy density of baryon and $\rho_m = \rho_b + \rho_\chi$. The term u_{th} is the variance of the relative velocity between DM and baryon and this is estimated as $u_{th} \equiv \sqrt{T_b/m_b + T_\chi/m_\chi}$. Following Ref. [16] we consider that the interaction cross-section σ is parametrized as $\sigma = \sigma_0 v^{-4}$. We note that σ_0 depends on the DM mass m_χ and this is scaled as $\sigma_0 = (m_\chi/\text{GeV}) \times 10^{-42} \text{ cm}^2$. The another unknown quantity $V_{\chi b}$ in Eq. 8 is the drag term of the relative velocity between DM and baryon.

III. RESULTS

In this analysis we consider a particle dark matter candidate in the framework of Inert Doublet Model (IDM) and estimate the dark matter annihilation cross-section and the relic density. From LHC experimental results, one sees that a range of relic densities can be obtained for IDM dark matter candidate. Here we estimate the relic density for the DM candidates which are divided mainly in two regions, *viz.* (a) $10 \text{ GeV} \leq M_{DM} \leq 80 \text{ GeV}$ and (b) $M_{DM} \geq 550 \text{ GeV}$. We see that the estimated relic densities for the different DM masses lie within the 95% confidence limit of the observed relic density obtained from the Planck Experiment [13], which is $\Omega_{c,0} = 0.120 \pm 0.001$. We use micrOMEGAs² [22] to estimate relic densities and corresponding annihilation cross-sections in case of dark matter candidate in IDM model for different DM masses. Some selected values of DM masses and the corresponding annihilation cross-section are tabulated in Table I.

Figure 1 shows the annihilation cross-section $\langle \sigma v \rangle$ for different DM masses M_χ for which the estimated relic densities Ω_c lie within the 95% confidence limit of the observed relic density $\Omega_{c,0}$ obtained from the Planck experiment. The curve does not fit with any particular mathematical function. However it gives an idea about the range of Ω_c (shaded region). For a fixed DM mass, one may choose for which the qualitative nature of the fluctuation in the 21-cm signal (δT_{21}) will not change significantly.

¹ <https://faun.rc.fas.harvard.edu/epsilon/>

² <https://lapth.cnrs.fr/micromegas/>

M_χ (GeV)	Ω_c	$\langle\sigma v\rangle$ cm ³ s ⁻¹
10	0.124	6.50×10^{-29}
20	0.116	7.72×10^{-29}
30	0.114	9.98×10^{-29}
40	0.116	1.65×10^{-28}
50	0.115	4.37×10^{-28}
60	0.124	1.40×10^{-27}
70	0.123	1.59×10^{-26}
80	0.113	2.59×10^{-26}
550	0.115	6.68×10^{-26}
990	0.113	4.88×10^{-26}

TABLE I. The relic density (Ω_c) and the corresponding annihilation cross-section ($\langle\sigma v\rangle$) for different dark matter masses (M_χ) for which the values of Ω_c lie within 95% confidence limit of $\Omega_{c,0}$ obtained from the Planck experiment.

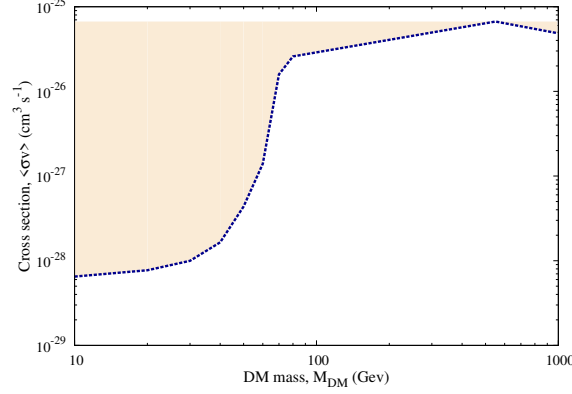


FIG. 1. Annihilation cross-section ($\langle\sigma v\rangle$) for the different dark matter mass (M_χ). The shaded region denotes the range of $\langle\sigma v\rangle$ one may choose for a fixed dark matter mass.

Our purpose is to show the effects of dark matter annihilation and DM-baryon elastic scattering on δT_{21} separately. This is given in Figure 2 and described above. The left panel of Figure 2 shows the fluctuation in the 21-cm brightness temperature (δT_{21}) at different redshift by considering DM annihilation as an additional effects on δT_{21} along with thermal evolution. Different color curves correspond to different DM masses mentioned in the figure. We find that for DM annihilation case (left panel of Figure 2), δT_{21} is minimum at different red shifts for different DM masses. However they lie within the redshift range $15 \leq z \leq 30$ for the DM mass range $10 \text{ GeV} \leq M_\chi \leq 990 \text{ GeV}$.

The DM annihilation produces heating effect on the baryon. This directly injects energy to the baryon and as a result the baryon temperature T_b increases. The increment in T_b further increases the spin temperature T_S and as a consequence the fluctuation in 21-cm signal δT_{21} gets modified. The energy injection to the baryon due to the DM annihilation is directly proportional to the ratio $\langle\sigma v\rangle/M_\chi$. This implies that δT_{21} is more negative for small $\langle\sigma v\rangle/M_\chi$. This feature is also evident in our analysis. The left panel of Figure 2 shows that we have highest negative value of δT_{21} for the DM mass $M_\chi = 30 \text{ GeV}$ where $\langle\sigma v\rangle/M_\chi = 3.33 \times 10^{-30} \text{ cm}^3 \text{ s}^{-1} \text{ GeV}^{-1}$ and we have the lowest negative value of δT_{21} for the DM mass $M_\chi = 80 \text{ GeV}$ where $\langle\sigma v\rangle/M_\chi = 3.24 \times 10^{-28} \text{ cm}^3 \text{ s}^{-1} \text{ GeV}^{-1}$.

The right panel of Figure 2 shows δT_{21} at different redshift by considering DM-baryon elastic scattering as an another additional effects on δT_{21} along with the thermal evolution. Different color lines correspond to different DM mass mentioned in the figure. For all the DM masses considered here we see that the value of δT_{21} is lowest at a particular redshift $z \approx 100$. However different lines almost overlap with each other for $z < 80$ and $z > 120$. For $80 \leq z \leq 120$ we find that δT_{21} are different for the different DM masses with δT_{21} minimum for $M_\chi = 10 \text{ GeV}$ and maximum for $M_\chi = 990 \text{ GeV}$. DM-baryon elastic scattering heats up the baryon due to the relative velocity between them and the baryon temperature T_b increases, which further modifies δT_{21} . We find that δT_{21} depends on the DM mass M_χ and the velocity drag term $V_{\chi b}$ for both the higher and lower DM masses. In Ref. [16], only lower DM masses are taken into consideration.

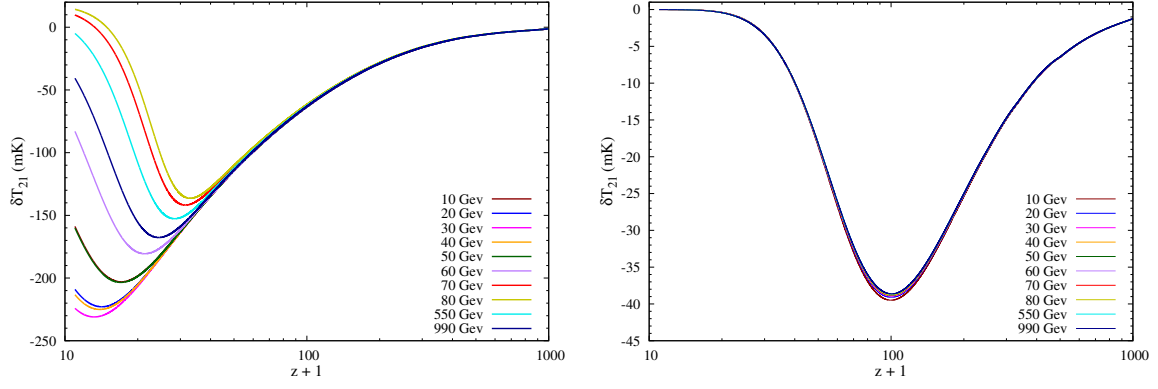


FIG. 2. The fluctuation in the 21-cm brightness temperature δT_{21} at different redshifts by considering the DM annihilation (left panel) and the DM-baryon elastic scattering (right panel) as an additional effect to δT_{21} apart from the thermal evolution. Different color lines correspond to different DM masses mentioned in the figure.

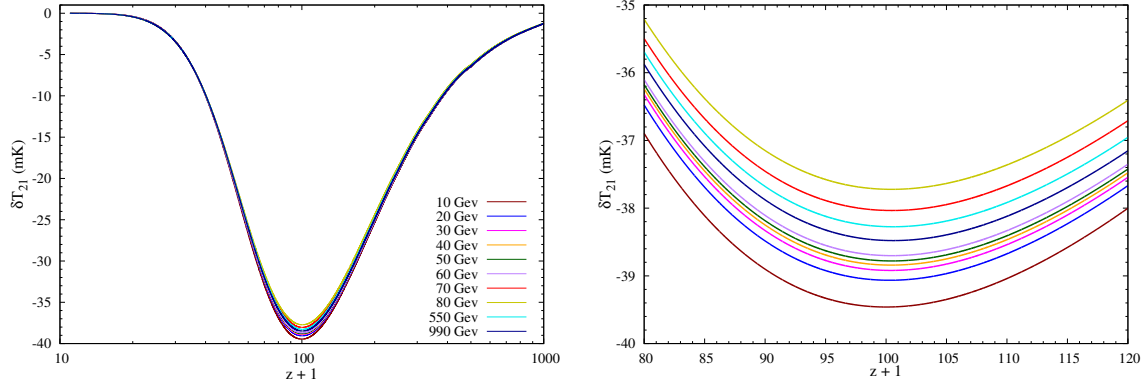


FIG. 3. The fluctuations in the 21-cm absorption lines δT_{21} (left panel) by considering both DM annihilation and DM-baryon elastic scattering as additional effects on δT_{21} along with the thermal evolution. Different color lines correspond to different DM mass mentioned in the figure. The right panel shows the zoomed version of the figure at left panel for $80 \leq z \leq 120$.

So far, we treat both the DM annihilation and DM-baryon elastic scattering as a combined effect on δT_{21} by simply adding them. The left panel of Figure 3 shows the variation of δT_{21} different redshift and different values of DM masses. In order to better understand the variations of δT_{21} due to combined effects of DM annihilation and scatterings for different dark matter masses. We show, in the right panel of Figure 3 a magnified version of the same but for the redshift range $80 \leq z \leq 120$. For different DM masses we see that δT_{21} is lowest at a particular redshift $z \approx 100$ and the value of δT_{21} almost overlap for different M_χ at $z < 60$ and $z > 150$. However for $80 \leq z \leq 120$ (right panel) it is evident that the values of δT_{21} are different for the different DM masses. We observe that δT_{21} is minimum for $M_\chi = 10$ GeV and maximum for $M_\chi = 80$ GeV. Note that these values are different if only annihilation or only scattering effects are taken into consideration.

It is seen that for the lower DM mass, i.e. $10 \text{ GeV} \leq M_\chi \leq 60 \text{ GeV}$, δT_{21} follows M_χ , whereas for the higher DM mass, i.e. $70 \text{ GeV} \leq M_\chi \leq 990 \text{ GeV}$, δT_{21} follows $\langle \sigma v \rangle / M_\chi$. However the DM-baryon elastic scattering is the most dominating part on δT_{21} . This feature can be explained as follows. For $40 \leq z \leq 200$, the baryons cool adiabatically in the absence of any DM interaction but in the presence of DM annihilation and DM-baryon elastic scattering the baryon will heat up and T_b increases accordingly although the value of $T_S - T_\gamma$ is still a small negative number.

Further more for the lower mass range ($10 \text{ GeV} \leq M_\chi \leq 60 \text{ GeV}$) the instantaneous energy deposition dominates and boost factor becomes effective for DM annihilation and for this reason at $z \sim 100$ we see the effect of instantaneous energy deposition at the lower mass range. However DM-baryon elastic scattering is always prominent here. For the higher mass range ($70 \text{ GeV} \leq M_\chi \leq 990 \text{ GeV}$) the delayed energy deposition takes over at $z \sim 100$ and as a consequence boost factor does not significantly contribute here. However at $z \sim 100$ the quantitative nature of δT_{21} for $M_\chi = 70, 80, 550$ and 990 GeV follows the DM annihilation contributions.

As mentioned earlier, the elastic scattering between DM and baryons with different temperature tends to keep

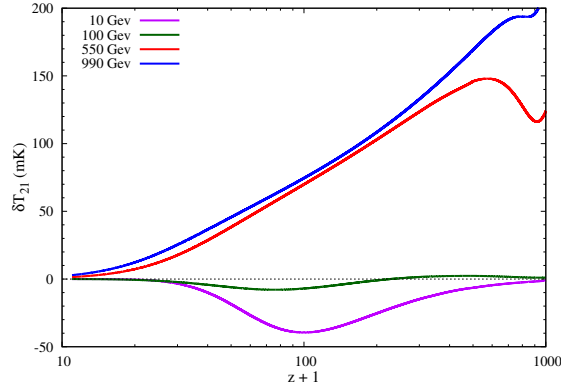


FIG. 4. The fluctuation on 21-cm brightness temperature for the DM masses mentioned in the figure for which the relic densities are not comparable with the relic density obtained from the Planck experiment.

M_χ (GeV)	Ω_c	$\langle\sigma v\rangle$ cm ³ s ⁻¹
10	2.72×10^1	6.50×10^{-29}
100	2.06×10^{-3}	1.54×10^{-24}
550	1.52×10^{-6}	9.43×10^{-22}
990	2.41×10^{-8}	1.11×10^{-20}

TABLE II. The relic density (Ω_c) and annihilation cross-sections ($\langle\sigma v\rangle$) for the different DM mass (M_χ) for which the values of Ω_c are not comparable with $\Omega_{c,0}$ obtained from the Planck experiment.

their temperature in equilibrium by heating up the cold DM where the heating rate depends on their temperature difference. But if there is a relative velocity between them then both DM and baryons are heated up due to the friction term. This creates an additional fluctuation on δT_{21} which is easier to detect as the energy deposition in this effect is large enough in comparison to that for the case of DM annihilation.

In order to investigate the behaviour of δT_{21} with the redshift in case when the dark matter mass does not satisfy the Planck relic density conditions we randomly choose a number of mass values for dark matter and the annihilation cross-section within the framework of IDM model which do not satisfy the Planck relic density conditions and compute the evolution of δT_{21} for those chosen masses and corresponding annihilation cross-sections. To this end we have chosen four different masses for the dark matter candidate namely $M_\chi = 10, 100, 550, 990$ GeV. These are tabulated in Table II. Note that these M_χ values are also used for Figs. 2 and 3 but for that case the IDM model parameters are so constrained that the Planck relic density is satisfied within 95% C.L. for each of the cases. The corresponding annihilation cross-section values and model parameters are used to compute δT_{21} for computing results shown in Figs. 2 and 3. But in this case arbitrary choice of model parameters are made and annihilation cross-sections and relic densities are obtained using those choices. It is obvious from Table II that calculated relic densities do not satisfy Planck results. We now investigate the deviation in the behaviour of δT_{21} with such choices.

The computed results for variations of δT_{21} with z for the above mentioned scenario is plotted in Figure 4. In Figure 4, we see that the qualitative nature of δT_{21} for $M_\chi = 100, 550$ and 990 GeV are totally different from the δT_{21} results when the relic densities lie within the 95% confidence limit of $\Omega_{c,0}$. For $M_\chi = 10$ GeV Table II shows that the annihilation cross-section is exactly equal to the same for the earlier case (Table I), however the relic densities are different. Most interestingly in Figure 4, we find that for $M_\chi = 100, 550$ and 990 GeV the value of δT_{21} is positive which implies that for this particular case we have 21-cm emission spectra rather than absorption spectra as in the earlier cases. The qualitative nature of δT_{21} for $M_\chi = 10$ GeV for both the cases are same due to the same annihilation cross-section $\langle\sigma v\rangle$ though there is a difference between the relic densities. The relic density of the DM should satisfy the abundance of Dark Matter determined by the Planck experiment. Considering this phenomenon, we can draw a lower bound on the annihilation cross-section $\langle\sigma v\rangle$ for different values of M_χ for the evolution of brightness temperature of 21-cm line at the dark ages when the contribution of DM through both the DM annihilation and the DM-baryon elastic scattering are taken into account. The shaded region of Figure 1 shows this lower bound on the annihilation cross-section $\langle\sigma v\rangle$ for different DM masses for which the qualitative nature of δT_{21} is similar to what is expected.

IV. SUMMARY AND DISCUSSION

Recent EDGES experiment [6] shows a strong 21-cm absorption spectra within the redshift range $14 < z < 20$ and gives the value of δT_{21} at $z = 17.2$. However the baryon temperature T_b , estimated from this experiment is far below the actual T_b estimated from Λ CDM cosmology. This discrepancy can be explained by either the colder than the expected values of T_b or the additional sources in the fluctuation of 21-cm brightness temperature. In this analysis we have considered two additional effects in δT_{21} , *viz.* DM annihilation and DM-baryon elastic scattering along with thermal evolution.

For DM annihilation the energy is deposited to the system either by instantaneous deposition or by delayed deposition. We have seen that for the instantaneous energy deposition, the boost factor become operational, however for the delayed energy deposition there is no such prominent effect of boost factor. Neglecting Wouthuysen-Field effect [5] we have estimated the relation between spin temperature T_S and baryon temperature T_b . The evolution in T_b has three major contributions from thermal evolution, DM annihilation and DM-baryon elastic scattering. We have used the formalism prescribed by [14] to estimate the DM annihilation contribution to T_b . Further we have also consider the formalism prescribed by [16] to estimate effect of DM-baryon elastic scattering to T_b . After estimating T_b we have finally calculated δT_{21} for the combined effect of the individual processes mentioned above.

We have considered IDM and used micrOMEGAs code [22] in order to estimate the DM annihilation cross-section and the corresponding relic density for a given IDM DM mass. Our analysis is basically divided in two cases of DM mass and annihilation cross-section where (1) the estimated relic densities (Ω_c) lie within the 95% confidence limit of the relic density ($\Omega_{c,0}$) obtained from the Planck experiment [13] and (2) the estimated relic densities are not comparable with $\Omega_{c,0}$. For the case (1) we have seen the absorption spectra of δT_{21} whereas for the case (2) we have seen the emission spectra of δT_{21} . This helps us to draw a lower bound on the DM annihilation cross-section by considering the fact that the relic density of the DM should be satisfied the abundance of Dark Matter determined by the Planck experiment. The lower bound of the annihilation cross-section lie within the range $\langle\sigma v\rangle \sim (6.5 \times 10^{-29}) - \sim (4.88 \times 10^{-26}) \text{ cm}^3/\text{sec}$ for the DM mass range $M_\chi \sim 10 - 990 \text{ GeV}$.

We have further noticed that the nature of δT_{21} for the lower DM masses, *i.e.* $10 \text{ GeV} \leq M_\chi \leq 60 \text{ GeV}$, follows the feature of DM-baryon elastic scattering and this is governed by M_χ . The nature of δT_{21} for the higher DM masses, *i.e.* $70 \text{ GeV} \leq M_\chi \leq 990 \text{ GeV}$, follows the DM annihilation and this is governed by $\langle\sigma v\rangle/M_\chi$. However for all the DM masses considered here the DM-baryon elastic scattering is the most prominent effect rather than the DM annihilation.

V. ACKNOWLEDGEMENT

Two of the authors (R.B. and S.B.) wish to acknowledge the support received from St. Xavier's College, Kolkata. One of the authors (R.B.) also thanks the Women Scientist Scheme-A fellowship (SR/WOS-A/PM-49/2018), Department of Science & Technology (DST), Govt. of India, for providing financial support. One of the author (M.P.) thanks the DST-INSPIRE Fellowship grant (DST/INSPIRE/FELLOWSHIP/[IF160004]) by DST Govt. of India. It is our pleasure to thank Siddhartha Bhattacharyya and Ashadul Halder for useful discussions and comments that greatly improved the manuscript.

-
- [1] J. R. Pritchard and A. Loeb, Phys. Rev. D **78**, 103511 (2008).
 - [2] J. R. Pritchard and A. Loeb, Reports on Progress in Physics **75**, 086901 (2012).
 - [3] M. Zaldarriaga, S. R. Furlanetto, and L. Hernquist, Astrophys. J. **608**, 622 (2004).
 - [4] G. B. Field, Proceedings of the IRE **46**, 240 (1958).
 - [5] C. M. Hirata, Mon. Not. R. Astr. Soc. **367**, 259 (2006).
 - [6] J. D. Bowman, A. E. E. Rogers, R. A. Monsalve, T. J. Mozdzen, and N. Mahesh, Nature **555**, 67 (2018).
 - [7] S. R. Furlanetto, S. Peng Oh, and F. H. Briggs, Phys. Rep. **433**, 181 (2006).
 - [8] A. Natarajan and D. J. Schwarz, Phys. Rev. D **80**, 043529 (2009).
 - [9] L. Lopez Honorez and C. E. Yaguna, JHEP **09**, 046 (2010).
 - [10] S. Banerjee, F. Boudjema, N. Chakrabarty, G. Chalons, and H. Sun, Phys. Rev. D **100**, 095024 (2019).
 - [11] J. Kalinowski, W. Kotlarski, T. Robens, D. Sokolowska, and A. F. Żarnecki, JHEP **12**, 81 (2018).
 - [12] V. M., F. A., M. M., and E. Ripamonti, Mon. Not. R. Astr. Soc. **377**, 245 (2007).
 - [13] P. Collaboration, A&A **641**, A6 (2020).
 - [14] G. D'Amico, P. Panci, and A. Strumia, Phys. Rev. Lett. **121**, 011103 (2018).
 - [15] H. Liu and T. R. Slatyer, Phys. Rev. D **98**, 023501 (2018).

- [16] J. B. Muñoz, E. D. Kovetz, and Y. Ali-Haïmoud, *Phys. Rev. D* **92**, 083528 (2015).
- [17] C. Dvorkin, K. Blum, and M. Kamionkowski, *Phys. Rev. D* **89**, 023519 (2014).
- [18] S. R. Furlanetto and M. R. Furlanetto, *Mon. Not. R. Astr. Soc.* **374**, 547 (2007).
- [19] A. Lewis and A. Challinor, *Phys. Rev. D* **76**, 083005 (2007).
- [20] T. R. Slatyer, *Phys. Rev. D* **93**, 023527 (2016).
- [21] T. R. Slatyer, *Phys. Rev. D* **93**, 023521 (2016).
- [22] G. Bélanger, F. Boudjema, A. Goudelis, A. Pukhov, and B. Zaldivar, *Computer Physics Communications* **231**, 173 (2018).